Nontraditional Constant Pressure Filtration Behavior

Anthony D. Stickland, Ross G. De Kretser, and Peter J. Scales
Particulate Fluids Processing Centre, Dept. of Chemical and Biomolecular Engineering, University of Melbourne, 3010, Australia

DOI 10.1002/aic.10501
Published online June 20, 2005 in Wiley InterScience (www.interscience.wiley.com).

Pressure filtration is a common industrial process used for solid–liquid separation and laboratory technique used to measure the compressional rheological properties of suspensions. Traditional approaches to the modeling of constant pressure filtration behavior of particulate systems stipulate quadratic behavior of time with filtrate volume. However, this is not necessarily a fundamental attribute of pressure filtration, but rather a result of the assumptions made of the compressibility and permeability of the material. This work solves diffusion-type constant pressure filtration governing equations using a finite-difference technique to demonstrate that filtration, under certain circumstances, is expected to show negligible quadratic behavior. Materials that exhibit such behavior have often been classified as nontraditional and methodologies have been developed to interpret such trends. This work illustrates that such behavior is in fact covered by extant filtration models and does not require any extra interpretation of the forces involved. Furthermore, it is shown that traditional or nontraditional behavior is dependent on the initial solids concentration and the applied pressure, such that the filtration of a suspension may show relatively long cake formation times at low initial concentrations or pressures, and relatively short times at high initial concentrations or pressures. © 2005 American Institute of Chemical Engineers *AIChE J,* 51: 2481–2488, 2005
Keywords: constant pressure filtration, solid/liquid separation, compressibility, permeability, solids diffusivity

Introduction

Understanding the behavior of solid–liquid systems in dewatering is important to many industries involving a range of processes from the thickening of minerals tailings to the ultrafiltration of proteins. The dewatering behavior in filtration, thickening, and centrifugation is described well by compressional rheology in which the equilibrium extent and rate of separation are determined by the compressibility and permeability, respectively. The compressibility and permeability of particulate systems are typically measured using a pressure filtration cell by recording the volume of filtrate with time.[1]

Models of constant pressure filtration[2-5] indicate that the filtration time t is quadratic with the specific filtrate volume V, during cake formation, followed by a logarithmic dependency (to first order) during cake compression. An example of a typical dead-end filtration experimental curve is shown in Figure 1, with a guideline to illustrate the quadratic behavior. The permeability can be determined from the slope of the t vs. V^2 linear section, and a measure of the compressibility from the equilibrium height.[6] Multiple-pressure tests are one method used to give the material characteristics over a range of solids concentrations (measured as solids volume fraction, ϕ) in a relatively short timescale.[7]

A wide range of particulate suspensions from the minerals, water, pigments, and ceramics industries (many of them flocculated) show filtration behavior typified by long cake formation times (up to 85% of the total time) followed by short

Correspondence concerning this article should be addressed to P. J. Scales at peterjs@unimelb.edu.au.

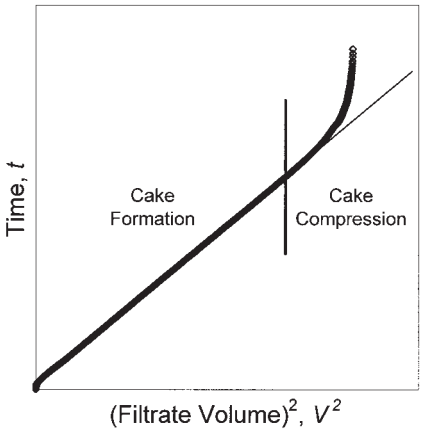

Figure 1. Example of experimental results for traditional filtration.

compression times. Indeed, the extraction of the parameters used in filtration prediction usually relies on this behavior. The term "traditional " is used in this work to describe relatively long cake formation times.

On the other hand, very different filtration profiles are observed for many sludges containing high molecular weight and crosslinked biomolecules,[8-10] including waste materials from the dairy industry or starch-rich sludges. These materials are sometimes classed as "supercompactable." [11] In constant pressure filtration, such sludges tend to show little or no cake formation followed by a long compression phase, as illustrated in Figure 2. Such behavior is termed "nontraditional " in this work.

For the data shown in Figure 2, it is difficult to extract permeability or compressibility parameter information from a single pressure run. Traditional filtration methods of using the slope of the linear section of the plot to extract parameters such as the hindered settling function or specific cake resistance (both related to the permeability) are inaccurate, given that short formation times and equilibrium compressibility data are obtained only after extremely long filtration times. Errors ascribed to evaporation and/or ageing of the sludge then compete with the accuracy of the compressibility determination. Thus,

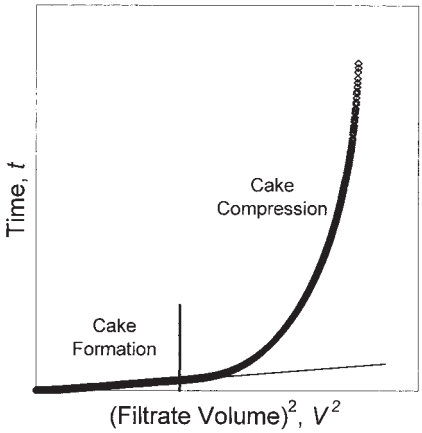

Figure 2. Example of experimental results for nontraditional filtration behavior.

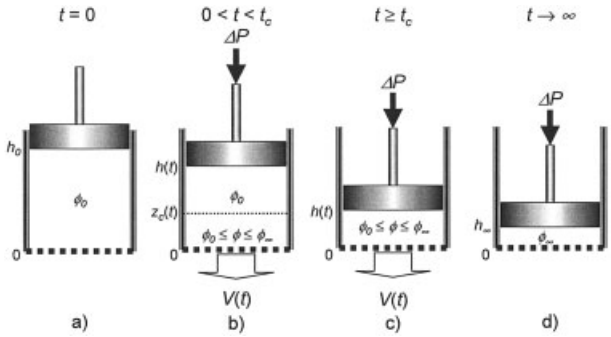

Figure 3. 1-D pressure filtration ($\phi_0 > \phi_g$).

multiple- or stepped-pressure techniques are unsound. Casagrande's log-time method for the determination of the consolidation coefficient c_v cannot be used because of the assumption of small strains.[12]

In recent work, Tiller and coworkers[13] measured the volume-average material properties of solidosity, permeability, and specific cake resistance using a stepped-pressure permeation technique, and define a class of materials as supercompactable based on the parameters used for the functional forms of the properties. As well as the difficulties using a multiple-pressure technique, the application of average properties over large volume fraction changes can be misleading,[14] and the theoretical approach requires empirical constitutive equations to be known *a priori*.

Aside from experimental difficulties associated with dewatering parameter determination, the question arises as to whether extant theory is capable of predicting such nontraditional behavior or whether extra forces are involved. An exemplary approach invoking extra forces is the recent approach used by Keiding and Rasmussen,[15] where a term postulated as being attributed to the osmotic pressure of the filter cake was used in a phenomenological description of nontraditional filtration.

The key purpose of this work is to dispel the myth that the mechanics of filtration for supercompactable materials are different from other particulate materials by exploring the circumstances when the theory of Landman and White,[16] solved using a computational numerical method, is capable of predicting nontraditional constant pressure filtration behavior.

Theory

Figure 3 shows a one-dimensional (1-D) pressure filtration. A suspension of initial solids volume fraction ϕ_0 is loaded into a filtration cell. A piston at height $h(t)$ is used to apply a pressure to the suspension to force water through a semipermeable membrane. Consolidation occurs and water is exuded until the material reaches its equilibrium compressibility limit ϕ_∞, for the given applied pressure ΔP. Buscall and White[17] presented a phenomenological model of solid–liquid separation in which the hindered settling factor $R(\phi)$ and the compressive yield stress $P_y(\phi)$ are local solids volume fraction–dependent parameters, allowing the situation to be described by a diffusion-type partial differential equation. $R(\phi)$ is a measure of the hydrodynamic drag between the fluid and the particles. $P_y(\phi)$ is a measure of the particulate network strength—a network is able to withstand a certain load, and fails if the load is ex-

ceeded. Thus, $P_y(\phi)$ gives the compressibility limit in pressure filtration: $P_y(\phi_\infty) = \Delta P$. $P_y(\phi)$ is zero for concentrations below the gel point ϕ_g, which is the concentration at which a network forms.

By balancing the mass and momentum equations of two-phase flow in solid–liquid separation, the overall governing equation for constant pressure filtration is given by the following partial differential equation[5]

$$\frac{\partial \phi}{\partial t} = \frac{\partial}{\partial z}\left[D(\phi)\,\frac{\partial \phi}{\partial z} - \phi\,\frac{dh(t)}{dt}\right] \tag{1}$$

Gravity is assumed to be negligible in Eq. 1, which is valid for most flocculated systems where gravity-settling timescales are much larger than pressure-filtration timescales.[16] The solids diffusivity $D(\phi)$ gives an overall measure of the dewaterability of a material and is analogous to the consolidation coefficient c_v, used by geotechnical engineers. It is defined by the ratio of the compressibility [as $dP_y(\phi)/d\phi$] and $R(\phi)$

$$D(\phi) = \frac{dP_y(\phi)}{d\phi}\,\frac{(1-\phi)^2}{R(\phi)} \tag{2}$$

The initial and boundary conditions for the problem are stated as follows

$$P_y[\phi(0, t)] = P_y(\phi_\infty) = \Delta P \tag{3}$$

$$\frac{\partial \phi}{\partial z}\,[h(t), t] = 0 \tag{4}$$

$$\phi(z, 0) = \phi_0 \tag{5}$$

Equation 3 is derived[5,16] by combining the particle and fluid pressures at the membrane and assuming that the membrane resistance R_m is zero (such that the fluid pressure is zero). This is a reasonable assumption for impermeable suspensions and clean membranes, given that R_m is negligible compared to the resistance of the cake.[18,19] Equation 4 is a consequence of equal solid and liquid velocities at the piston, indicating that there is a moving boundary condition at the piston, given that h is a function of t. The initial condition (Eq. 5) contradicts the boundary condition at the membrane (Eq. 3), indicating that the solution also has an internal moving boundary condition at $z_c(t)$. This internal boundary represents the top of the cake. Material above the cake is at the initial concentration: $\phi(z > z_c) = \phi_0$. For $\phi_0 < \phi_g$, the top of the cake is discontinuous (that is, there is an abrupt change in concentration from the top of the cake to the bulk suspension), with $\phi(z_c^-, t) = \phi_g$ and $d\phi/dz \geq 0$. For $\phi_0 > \phi_g$, the top of the cake is continuous [$\phi(z_c^-, t) = \phi_0$ and $d\phi/dz = 0$]. For the case when $\phi_0 > \phi_g$ and R_m is included, this internal boundary does not exist.[20] Only the $R_m = 0$, $\phi_0 > \phi_g$ case is considered here.

The overall conservation of particle volume is given by ϕ_0 and the initial piston height h_0, such that

$$\int_0^{h(t)} \phi(z, t)dz = \phi_0 h_0 \tag{6}$$

Change of variables

Landman and White[5] simplified the problem by scaling the parameters z, $h(t)$, and t to Z, $H(T)$, and T, respectively, converting Z to a material coordinate w, and substituting void ratio e, for ϕ such that

$$Z = \frac{z}{h_0} \tag{7}$$

$$H(T) = \frac{h(t)}{h_0} \tag{8}$$

$$T = \frac{tD_\infty}{h_0^2}\left(\frac{\phi_\infty}{\phi_0}\right)^2 \tag{9}$$

where

$$D_\infty = D(\phi_\infty) \tag{10}$$

The material coordinate w encompasses the entire filtration cell, such that $w(0, T) = 0$ and $w[H(T), T] = 1$, and is given by

$$w(Z, T) = \frac{1}{\phi_0}\int_0^Z \phi(Z, T)dZ \tag{11}$$

The void ratio (the ratio of the liquid volume to the solid volume) is related to the volume fraction by

$$e = \frac{1}{\phi} - 1 \tag{12}$$

The variable e should not be confused with the porosity ε, which is the ratio of the liquid volume to the total volume ($\varepsilon = 1 - \phi$). Using these substitutions (Eqs. 7–12), the problem is restated as a simpler second-order diffusion-type equation

$$\frac{\partial e}{\partial T} = \frac{\partial}{\partial w}\left[\Delta(e)\,\frac{\partial e}{\partial w}\right] \tag{13}$$

where

$$\Delta(e) = \frac{\phi^2 D(\phi)}{\phi_\infty^2 D_\infty} \tag{14}$$

The boundary and initial conditions are restated as

$$e(0, T) = e_\infty = \frac{1}{\phi_\infty} - 1 \tag{15}$$

$$\frac{\partial e}{\partial w}(1, T) = 0 \tag{16}$$

$$e(w, 0) = e_0 = \frac{1}{\phi_0} - 1 \tag{17}$$

Introducing w removes the moving boundary condition at the piston, but does not remove the internal moving boundary condition (Eqs. 15 and 17 still contradict each other).

Linear approximation

Landman and White[5] showed that by introducing an approximation for $\Delta(e)$, Δ_{eff}, the overall governing Eq. 13 has analytical solutions for cake formation and cake compression. The approximation for $\Delta(e)$ is to replace it with a step function of unit height Δ_{eff}

$$\Delta_{eff} = \theta(e^* - e) = \begin{Bmatrix} 1 & e \le e^* \\ 0 & e > e^* \end{Bmatrix} \tag{18}$$

Δ_{eff} effectively shifts the gel point to e^*, such that $\partial e/\partial T = 0$ for $e > e^*$. Because of the internal moving boundary, there are two regions: one of cake growth ($e \le e^*$) and one of constant concentration ($e = e_0$). The choice of e^* ensures that Δ_{eff} is scaled so that the value at e_∞ and the area under the $\Delta(e)$ curve from e_∞ to e_0 are preserved. The suggested form for e^* is

$$e^* = e_\infty + \int_{e_\infty}^{e_0} \Delta(e)de \tag{19}$$

Thus, the approximation is dependent on both e_0 and e_∞ and is therefore dependent on the operating conditions of ϕ_0 and ΔP. The corresponding approximation to $D(\phi)$, D_{eff}, given by combining Eqs. 14 and 18, is hyperbolic in nature

$$D_{eff} = \begin{Bmatrix} 0 & \phi < \phi^* \\ \dfrac{\phi_\infty^2 D_\infty}{\phi^2} & \phi \ge \phi^* \end{Bmatrix} \tag{20}$$

The solution indicates that before a critical time T_c, a cake forms above the membrane and H^2 is linear with T. At T_c the growing cake reaches the piston and the cake begins to compress. A Fourier series that is logarithmic to first order gives the solution in the compression region. The linear approximation has been shown to satisfactorily predict filtration for many materials, including mineral tailings,[21] clays,[18] and water-treatment sludges.[22,23] These materials generally show traditional behavior and exhibit increasing or constant $D(\phi)$ from ϕ_0 to ϕ_∞.

By this rationale, the filtration behavior is nontraditional when T_c is small relative to the overall filtration time. T_c must always be positive when $R_m = 0$ because there is always a finite time taken for the shock at (0, 0) to propagate to the piston. For $R_m \neq 0$, $\phi_0 > \phi_g$, T_c is zero. Thus, the linear approximation fails when $\phi^* < \phi_0$ because $T_c < 0$. For $T_c \ge 0$, $e^* \le e_0$. Thus, from Eq. 19

$$e_0 - e_\infty \le \int_{e_\infty}^{e_0} \Delta(e)de \tag{21}$$

A crude approximation to the integral is made using the trapezium rule

$$\int_{e_\infty}^{e_0} \Delta(e)de \approx \frac{e_0 - e_\infty}{2}[1 + \Delta(e_0)] \tag{22}$$

Thus, as a rule of thumb, $\Delta(e_0) > 1$, or $\Delta(e)$ must increase from e_∞ to e_0, for T_c to be small. Correspondingly, $D(\phi_0) > D_\infty(\phi_\infty/\phi_0)^2$ [that is, $D(\phi)$ significantly decreases] for the filtration behavior to show relatively short cake formation times. From the definition of $D(\phi)$ (Eq. 2), $dP_y(\phi)/d\phi$ must increase at a slower rate than $R(\phi)$ with increasing ϕ.

Although the linear approximation provides insight into the relative cake formation time, it is shown later that T_c is underestimated for certain conditions when ϕ^* decreases toward ϕ_0, which is precisely the area of interest in this work. As a result, a numerical algorithm using finite differences will be used to solve the filtration equation.

Finite-difference method

Finite-difference methods are well-established numerical methods requiring computational solution.[24] An explicit central difference approximation is used here to solve the governing equation. In explicit form, Eq. 13 becomes

$$\frac{\partial e}{\partial T} = \frac{\partial^2 \delta(e)}{\partial w^2} \tag{23}$$

where $\delta(e)$ is the integral of $\Delta(e)$

$$\delta(e) = \int \Delta(e)de \tag{24}$$

The material coordinate w is divided into J discrete lengths of Δw and the time dimension into N discrete steps of ΔT. The void ratio at time $n + 1$ and position j is given by Eq. 23 using a central difference approximation in Δw and a forward difference approximation in ΔT

$$e_{n+1,j} = e_{n,j} + \frac{\Delta T}{\Delta w^2}[\delta(e_{n,j+1}) - 2\delta(e_{n,j}) + \delta(e_{n,j-1})] \tag{25}$$

The initial and boundary conditions (Eqs. 15–17) in discrete form become

$$e_{n+1,0} = e_\infty \tag{26}$$

$$e_{n+1,J} = e_{n,J} - 2\frac{\Delta T}{\Delta w^2}[\delta(e_{n,J}) - \delta(e_{n,J-1})] \tag{27}$$

$$e_{0,j} = e_0 \tag{28}$$

The factor 2 in Eq. 27 arises from the central rather than the backward difference approximation to Eq. 16.[24] Equations 25–28 give a complete description of 1-D constant pressure filtration—if all the values of $e_{n,j}$ are known, the finite-difference equation can be solved for $e_{n+1,j}$. The void ratio distribution at time $n + 1$ is averaged over all j values to give the average volume fraction $\langle\phi\rangle_{n+1}$, the piston height h_{n+1}, and the specific filtrate volume V_{n+1}.

$$\langle\phi\rangle_{n+1} = \frac{1}{1 + \dfrac{1}{J+1}\displaystyle\sum_{j=0}^{J} e_{n+1,j}} \tag{29}$$

$$h_{n+1} = \frac{h_0\phi_0}{\langle\phi\rangle_{n+1}} \tag{30}$$

$$V_{n+1} = h_0 - h_{n+1} \tag{31}$$

The accuracy and required computational time of the finite-difference method depends on the size of the length step Δw (the accuracy is of order Δw^2) and thus the value that is chosen for the number of steps J. J is chosen to keep the error of the finite approximation small—in this case, $J = 100$. The time step ΔT is given by the convergence and stability criteria of the finite approximation[25]

$$\Delta T = r\frac{\Delta w^2}{\Delta(e_0)} \tag{32}$$

For the explicit scheme, $r \leq 1/2$ gives a local truncation error of order (ΔT) and (Δw^2),[24] which is the value chosen here.

Material Characteristics

The dewatering characteristics of a particulate system are presented as compressive yield stress $P_y(\phi)$ and hindered settling function $R(\phi)$. There are a number of functional forms used in the literature to describe these volume fraction–dependent functions. The power-law functions used in this paper are given by Eqs. 33 and 34,[16] but are chosen only to show a type of behavior in the material characteristics

$$P_y(\phi) = \begin{Bmatrix} 0 & \phi < \phi_g \\ p_1\left[\left(\dfrac{\phi}{\phi_g}\right)^{p_2} - 1\right] & \phi \geq \phi_g \end{Bmatrix} \tag{33}$$

$$R(\phi) = r_1(1 - \phi)^{r_2} \tag{34}$$

Substituting into Eq. 2 gives the solids diffusivity $D(\phi)$

$$D(\phi) = \begin{Bmatrix} 0 & \phi < \phi_g \\ d_1\phi^{d_2}(1 - \phi)^{d_3} & \phi \geq \phi_g \end{Bmatrix} \tag{35}$$

where

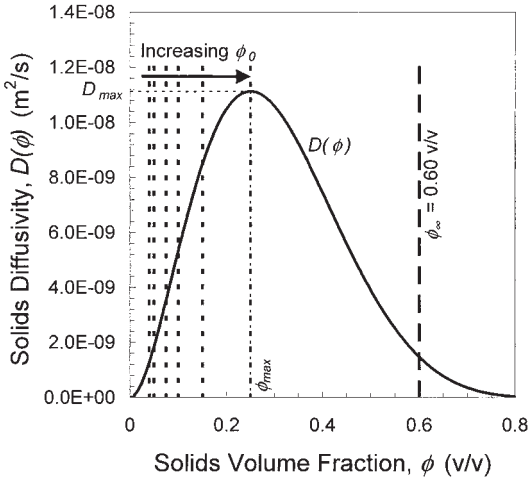

Figure 4. Plot of $D(\phi)$ showing ϕ_∞ and the range of ϕ_0 values used for modeling variable initial concentration.

$$d_1 = \frac{p_1p_2}{r_1\phi_g^{p_2}} \qquad d_2 = p_2 - 1 \qquad d_3 = 2 - r_2 \tag{36}$$

For this power-law functional form, $D(\phi)$ has a maximum (D_{max}) at ϕ_{max}, as shown in Figure 4

$$\phi_{max} = \frac{d_2}{d_3 + d_2} = \frac{p_2 - 1}{p_2 - r_2 + 1} \tag{37}$$

For many particulate systems, $D(\phi)$ has been shown to be monotonically increasing and the filtration behavior shows the traditional long cake formation and short cake compression.[18,21-23] This work investigates the consequences of $D(\phi)$ exhibiting a turning point or decreasing over the volume fraction range from ϕ_0 to ϕ_∞. For $D(\phi)$ to show this behavior, the $P_y(\phi)$ of the material must be a weak function of ϕ [that is, $dP_y(\phi)/d\phi$ is low] and $R(\phi)$ is a strong function of ϕ. Unpublished data from our laboratory suggest that suspensions of large crosslinked biomolecules such as sewage or dairy sludges, which have weak, deformable structures, exhibit such behavior. The parameters used in Eqs. 33 and 35, given in Table 1, are chosen to demonstrate a type of behavior rather than to explicitly predict a given filtration time. These values, based on a material with low permeability but high compressibility, are not representative of any particular material. From the parameters given in Table 1, ϕ_{max} is 0.250 v/v.

Table 1. Material Property Parameters

Parameter	Value
ϕ_g	0.01 v/v
p_1	1.00 Pa
p_2	3.00
d_1	1.00×10^{-6} m²/s
d_2	2.00
d_3	6.00

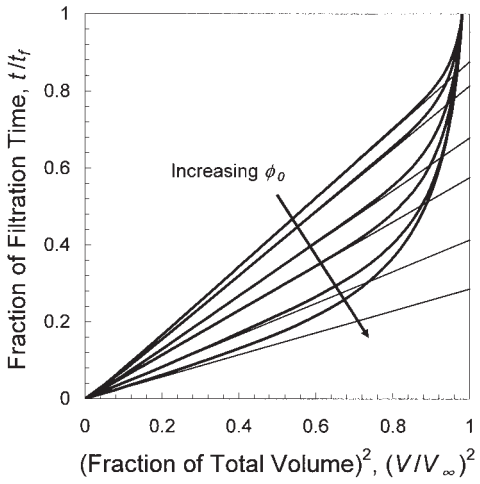

Figure 5. Finite-difference modeling predictions of constant pressure filtration for ϕ_∞ = 0.60 v/v with varying ϕ_0.

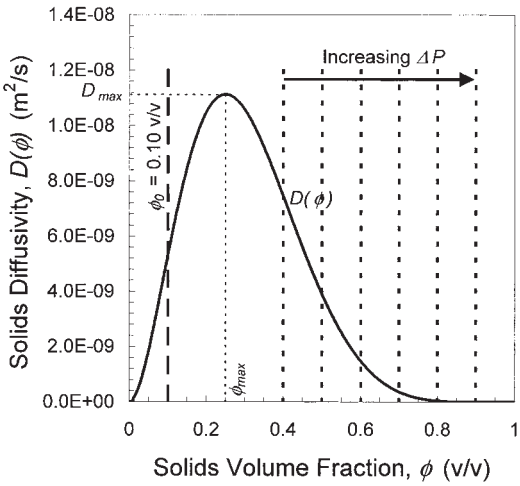

Figure 6. Plot of $D(\phi)$ showing ϕ_0 and the range of ϕ_∞ values used for modeling variable applied pressure.

Modeling Results

The filtration model is used in conjunction with the material characteristics above to generate results of t vs. V^2 for two scenarios:

(1) Variable ϕ_0 values with constant ΔP

(2) Variable ϕ_∞ values with constant ϕ_0

For illustration purposes, V is scaled with the equilibrium specific filtrate volume V_∞ and t is scaled with t_f, the time taken to reach a fraction f of V_∞ such that nontraditional behavior is observed when t/t_f vs. V/V_∞ deviates from linearity at early relative times. In the examples shown here, f is chosen as 0.99. V_∞ is given by a volumetric balance

$$V_\infty = h_0\left(1 - \frac{\phi_0}{\phi_\infty}\right) \tag{38}$$

where h_0 is constant at 0.04 m for all the examples. Varying h_0 would not affect the relative formation time, given that both t and V^2 vary with h_0^2.

Variable initial volume fraction

The finite-difference method is used to generate filtration curves at an applied pressure (ΔP) of 216 kPa (corresponding to a final volume fraction, ϕ_∞, of 0.6 v/v) for a range of initial concentrations, ϕ_0 = {0.04, 0.05, 0.075, 0.10, 0.15, 0.25} v/v. ϕ_0 is $>\phi_g$ to avoid the discontinuity at z_c. These ϕ_0 values are chosen to sample different portions of the $D(\phi)$ curve for use in the model (see Figure 4), with $D(\phi_0)$ values from less than D_∞ up to D_{max}, such that $D(\phi)$ is either increasing and then decreasing or predominantly decreasing.

The modeling results of t/t_f vs. $(V/V_\infty)^2$ for the range of ϕ_0 values are presented in Figure 5. Guidelines are shown to illustrate the deviation from linearity. The results clearly show that as ϕ_0 approaches ϕ_{max} and $D(\phi_0)$ increases, the filtration curves have shorter formation times and longer compression times, proving that the filtration theory can generate the nontraditional behavior under appropriate conditions without any extra interpretation of the forces involved.

Variable applied pressure

The other operating variable that has an effect on the relative cake formation time is the applied pressure. A plot of $D(\phi)$, ϕ_0 = 0.10 v/v, and ΔP = {63, 124, 215, 342, 511, 728} kPa is presented in Figure 6—the applied pressures correspond to ϕ_∞ = {0.40, 0.50, 0.60, 0.70, 0.80, 0.90} v/v. As with the case for variable ϕ_0, the ϕ_∞ values are chosen arbitrarily to sample different portions of the $D(\phi)$ curve, with D_∞ from close to D_{max} to less than $D(\phi_0)$.

The filtration predictions for variable applied pressure are shown in Figure 7. The results show that, as with the variable ϕ_0 case, relatively short formation times are also dependent on ΔP. Thus, a material that exhibits traditional filtration behavior at low pressures may become increasingly nontraditional as the pressure increases.

In general, for the model to give predictions with short formation times and long compression times, $D(\phi)$ decreases

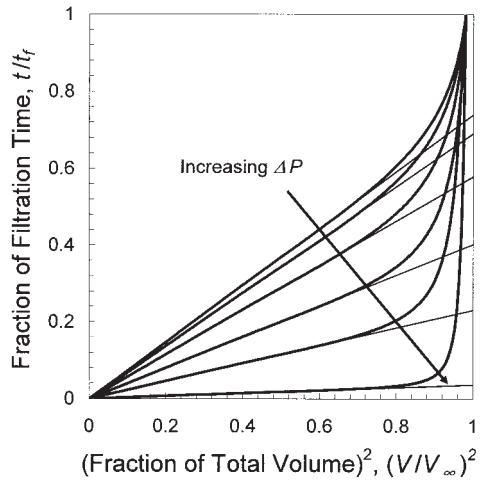

Figure 7. Finite-difference modeling predictions of constant pressure filtration for ϕ_0 = 0.10 v/v with varying applied pressure.

from ϕ_0 to ϕ_∞. This is attributed to high compressibility over the solids range, such that $D(\phi)$ has a weak dependency on $dP_y(\phi)/d\phi$ and a strong dependency on $R(\phi)$. Sludges with deformable, rearrangeable structures that contain high molecular weight and crosslinked biomolecules fit this description.

The finite-difference numerical solution is used for the above predictions instead of the linear approximation because the latter does not apply for ϕ^* values $< \phi_0$. There is also a region as ϕ^* decreases toward ϕ_0 where T_c is underestimated. This is illustrated in Figure 8, which shows a comparison of the predictions from the two methods for $\phi_0 = 0.1$ v/v, where, even though $\phi^* > \phi_0$, the linear approximation predicts an earlier cake compression.

The linear approximation is useful, however, for providing insight into the conditions required for relatively short formation times because nontraditional behavior is expected when $\phi^* < \phi_0$. A plot of ϕ^* calculated from Eq. 19 as a function of ϕ_0 for a range of applied pressures (see Figure 9) shows that, at constant initial concentrations, ϕ^* decreases with increasing pressure—thus higher pressures will be expected to show shorter relative formation times. For $\phi_0 = 0.10$ v/v, $\phi^* = \phi_0$ when $\phi_\infty = 0.621$ v/v. At constant pressure with $\phi_\infty = 0.60$ v/v, ϕ^* increases slowly with increasing ϕ_0 until $\phi^* = \phi_0 = 0.120$ v/v. Thus, the trends observed are the same as those given by the full numerical solution.

Conclusions

The solid–liquid separation theory of constant pressure filtration is solved using a finite-difference method and is shown to exhibit short formation times and long compression times when $D(\phi)$ decreases over the volume fraction range of interest. Rather than belonging just to a class of materials, such behavior is dependent on both the material properties and the operating conditions. The physical interpretation of this result is that materials that have deformable, rearrangeable structures will exhibit nontraditional constant pressure filtration behavior at high pressures and/or high initial concentrations. Significantly, no extra forces were invoked. Provided that the correct dewatering properties are obtained, the theory can predict nontraditional behavior—the challenge is now to more accurately determine these properties given that permeability and compressibility information is difficult to extract.

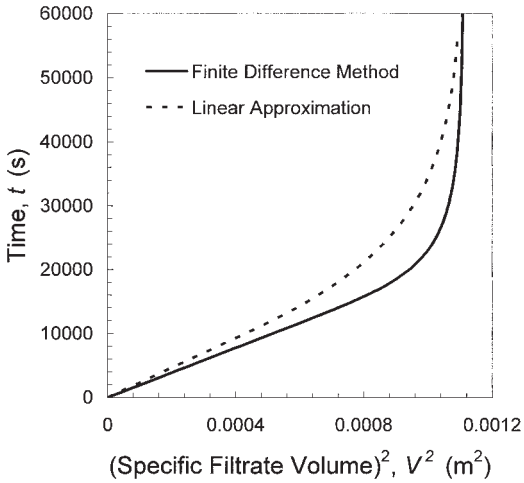

Figure 8. Linear approximation and finite-difference predictions for $\phi_\infty = 0.6$ v/v and $\phi_0 = 0.1$ v/v.

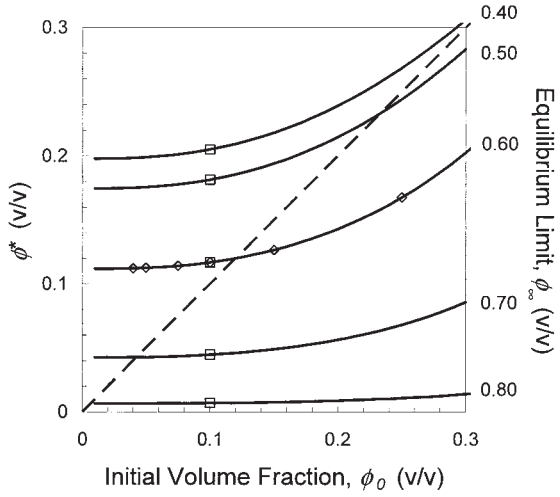

Figure 9. ϕ^* as a function of ϕ_0 for a range of ϕ_∞ values.

◇, Variable applied pressure; □, variable initial concentration; – – –, $\phi^* = \phi_0$.

Acknowledgments

The authors gratefully acknowledge the financial support of the Particulate Fluids Processing Centre (funded as a Special Research Centre of the Australian Research Council), Brisbane City Council (Australia), United Utilities (UK) and Yorkshire Water (UK). A.D.S. acknowledges receipt of an Australian Postgraduate Award from the Australian Research Council.

Notation

$D(\phi)$ = solids diffusivity
D_∞ = solids diffusivity at ϕ_∞
d_1, d_2, d_3 = diffusivity parameters
$e(w, T)$ = void ratio
f = stopping fraction
$h(t)$ = piston height
h_0 = initial piston height
$H(T)$ = scaled piston height
$P_y(\phi)$ = compressive yield stress
p_1, p_2 = compressibility parameters
$R(\phi)$ = hindered settling function
R_m = membrane resistance
r = finite-difference stability and convergence factor
r_1, r_2 = permeability parameters
t = filtration time
t_f = time of filtration to stopping fraction
T = scaled filtration time
T_c = scaled time to cake compression
$V(t)$ = specific filtrate volume
V_∞ = equilibrium specific filtrate volume
w = material coordinate
z = length coordinate
$z_c(t)$ = cake height
Z = scaled length coordinate

Greek letters

$\Delta(e)$ = scaled solids diffusivity (implicit)
$\delta(e)$ = scaled solids diffusivity (explicit)
ΔP = applied pressure
$\phi(z, t)$ = local solids volume fraction
ϕ_0 = initial solids volume fraction
ϕ_∞ = equilibrium solids volume fraction

ϕ_g = gel point volume fraction
ϕ^* = linear approximation effective gel point
$\langle\phi\rangle$ = average solids volume fraction

Literature Cited

1. Shirato M, Sambuichi M, Kato H, Aragaki H. Internal flow mechanism in filter cakes. *AIChE J*. 1969;15:405.
2. Ruth BF. Correlating filtration theory with industrial practice. *Ind Eng Chem*. 1946;38:564-571.
3. Tiller FM, Shirato M. The role of porosity in filtration: VI. New definition of filtration resistance. *AIChE J*. 1964;10:61-67.
4. Terzaghi K, Peck RB. *Soil Mechanics in Engineering Practice*. 2nd Edition. New York, NY: Wiley; 1967.
5. Landman KA, White LR. Predicting filtration time and maximizing throughput in a pressure filter. *AIChE J*. 1997;43:3147-3160.
6. Green MD, Landman KA, de Kretser RG, Boger DV. Pressure filtration technique for complete characterisation of consolidating suspensions. *Ind Eng Chem Res*. 1998;37:4152-4156.
7. de Kretser RG, Usher SP, Scales PJ, Boger DV, Landman KA. Rapid filtration measurement of dewatering design and optimisation parameters. *AIChE J*. 2001;47:1758-1769.
8. Tiller FM, Kwon JH. Role of porosity in filtration: XIII. Behavior of highly compactible cakes. *AIChE J*. 1998;44:2159-2167.
9. Anderson NJ, Dixon DR, Harbour PJ, Scales PJ. Complete characterisation of thermally treated sludges. *Water Sci Technol*. 2002;46:51-54.
10. Scales PJ, Dixon DR, Harbour PJ, Stickland AD. The fundamentals of waste water sludge characterization and filtration. Proc of the IWA Specialist Conference: BIOSOLIDS 2003, Wastewater Sludge as a Resource, Trondheim, Norway, June 23–25; 2003.
11. Tiller FM, Li WP. Strange behaviour of super-compactible filter cakes. *Chem Process*. 2000;63:49.
12. Casagrande A, Fadum RE. *Notes on Soil Testing for Engineering Purposes* (Harvard Soil Mechanics Series). Cambridge, MA: Harvard Univ. Press; 1940;8.
13. Tiller FM, Li WP, Lee JB. Determination of the critical pressure drop for filtration of super-compactible cakes. *Water Sci Technol*. 2001;44:171-176.
14. Lee DJ, Ju SP, Kwon JH, Tiller FM. Filtration of highly compactible filter cake: Variable internal flow rate. *AIChE J*. 2000;46:110-118.
15. Keiding K, Rasmussen MR. Osmotic effects in sludge dewatering. *Adv Environ Res*. 2003;7:641-645.
16. Landman KA, White LR. Solid/liquid separation of flocculated suspensions. *Adv Colloid Interface Sci*. 1994;51:175-246.
17. Buscall R, White LR. The consolidation of concentrated suspensions. Part 1. The theory of sedimentation. *J Chem Soc Faraday Trans 1*. 1987;83:873-891.
18. Eberl M, Landman KA, Scales PJ. Scale up procedures and test methods in filtration: A test case on kaolin plant data. *Colloids Surf A*. 1995;103:1-10.
19. Usher SP, de Kretser RG, Scales PJ. Validation of a new filtration technique for dewaterability characterization. *AIChE J*. 2001;47:1561-1570.
20. Landman KA, Sirakoff C, White LR. Dewatering of flocculated suspensions by pressure filtration. *Phys Fluids A*. 1991;3:1495-1509.
21. de Kretser RG, Scales PJ, Usher SP. Practically applicable modelling of cake filtration. Proc of Science & Technology of Filtration and Separations for the 21st Century, Tampa, FL, May; 2001.
22. Aziz AAA, de Kretser RG, Dixon DR, Scales PJ. The characterisation of slurry dewatering. *Water Sci Technol*. 2000;41:9-16.
23. Harbour PJ, Anderson NJ, Aziz AAA, Dixon DR, Hillis P, Scales PJ, Stickland AD, Tillotson M. Fundamental dewatering characteristics of potable water treatment sludges. *J Water Supply Res Technol Aqua*. 2004;53:29-36.
24. Smith GD. *Numerical Solution of Partial Differential Equations: Finite Difference Methods*. 3rd Edition. Oxford, UK: Oxford Univ. Press; 1985.
25. Matthews JH. *Numerical Methods for Mathematics, Science, and Engineering*. 2nd Edition. Englewood Cliffs, NJ: Prentice-Hall; 1992.

Manuscript received Jun. 2, 2004, and revision received Jan. 3, 2005.